Doctoral research design & a discussion on the paper "Strong contributions of local background climate to urban heat island"

Chang Cao

Video Conference

Yale-NUIST Center on Atmospheric Environment

Room 514, Meteorology Building, August 1st,2014

Doctoral research design

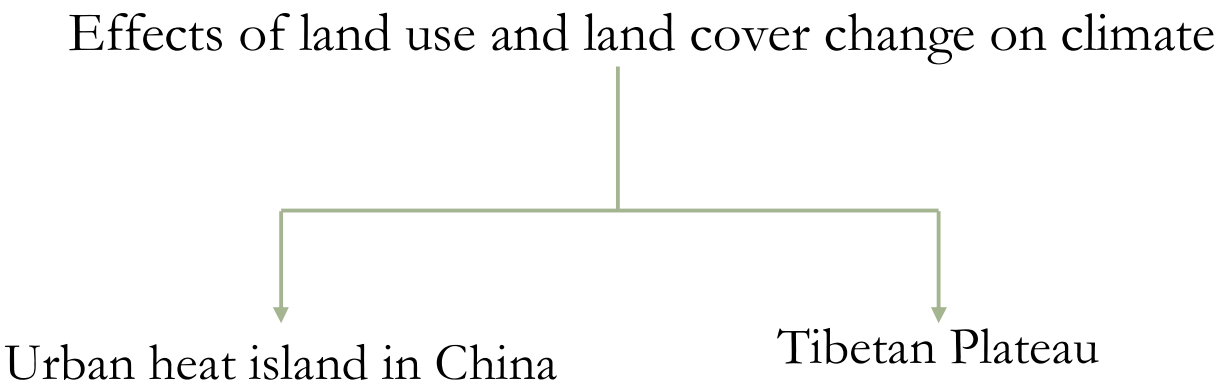

Discussion on a paper

LETTER

doi:10.1038/nature13462

Strong contributions of local background climate to urban heat islands

Lei Zhao[1,2], Xuhui Lee[1,2], Ronald B. Smith[3] & Keith Oleson[4]

The urban heat island (UHI), a common phenomenon in which surface temperatures are higher in urban areas than in surrounding rural areas, represents one of the most significant human-induced changes to Earth's surface climate[1,2]. Even though they are localized hotspots in the landscape, UHIs have a profound impact on the lives of urban residents, who comprise more than half of the world's population[3]. A barrier to UHI mitigation is the lack of quantitative attribution of the various contributions to UHI intensity[4] (expressed as the temperature difference between urban and rural areas, ΔT). A common perception is that reduction in evaporative cooling in urban land is the dominant driver of ΔT (ref. 5). Here we use a climate model to show that, for cities across North America, geographic variations in daytime ΔT are largely explained by variations in the efficiency with which urban and rural areas convect heat to the lower atmosphere. If urban areas are aerodynamically smoother than surrounding rural areas, urban heat dissipation is relatively less efficient and urban warming occurs (and vice versa). This convection effect depends on the local background climate, increasing daytime ΔT by 3.0 ± 0.3 kelvin (mean and standard error) in humid climates but decreasing ΔT by 1.5 ± 0.2 kelvin in dry climates. In the humid eastern United States, there is evidence of higher ΔT in drier years. These relationships imply that UHIs will exacerbate heatwave stress on human health in wet climates where high temperature effects are already compounded by high air humidity[6,7] and in drier years when positive temperature anomalies may be reinforced by a precipitation–temperature feedback[8]. Our results support albedo management as a viable means of reducing ΔT on large scales[9,10].

The conversion of natural land to urban land causes several notable perturbations to the Earth's surface energy balance. Reduction of evaporative cooling is generally thought to be the dominant factor contributing to UHI. Anthropogenic heat release is an added energy input to the energy balance and should increase the surface temperature. Energy input by solar radiation will also increase if albedo is reduced in the process of land conversion. Buildings and other artificial materials can store more radiation energy in the daytime than can natural vegetation and soil; release of the stored energy at night contributes to night-time

Background

- The Urban Heat Island (UHI) has great influence on local residents and regional climate.
- Impact factors:

$$R_n = (1-\alpha)K_{\downarrow} + L_{\downarrow} - L_{\uparrow} \qquad (1)$$

$$R_n + Q_{AH} = H + LE + Q_s \qquad (2)$$

Scientific questions

- What are the quantitative contributions of impact factors? Is evaporative cooling the driving factor of UHI?
- What is the effect of climatic context on UHI?

Method

- **Remote Sensing**
- MODIS-Aqua land surface temperature (8-day, 1km, 2003-2012)
- Night-time(1:30) and daytime (13:30) ΔT

- **Climate Model**
- Community Earth System Model (CESM)
- Resolution: 0.31° (latitude) × 0.23° (longitude)
- Clear day, 1:00 and 13:00, 1972-2004 (60yr spin-up)

(http://www.cesm.ucar.edu/models/ccsm4.0/)

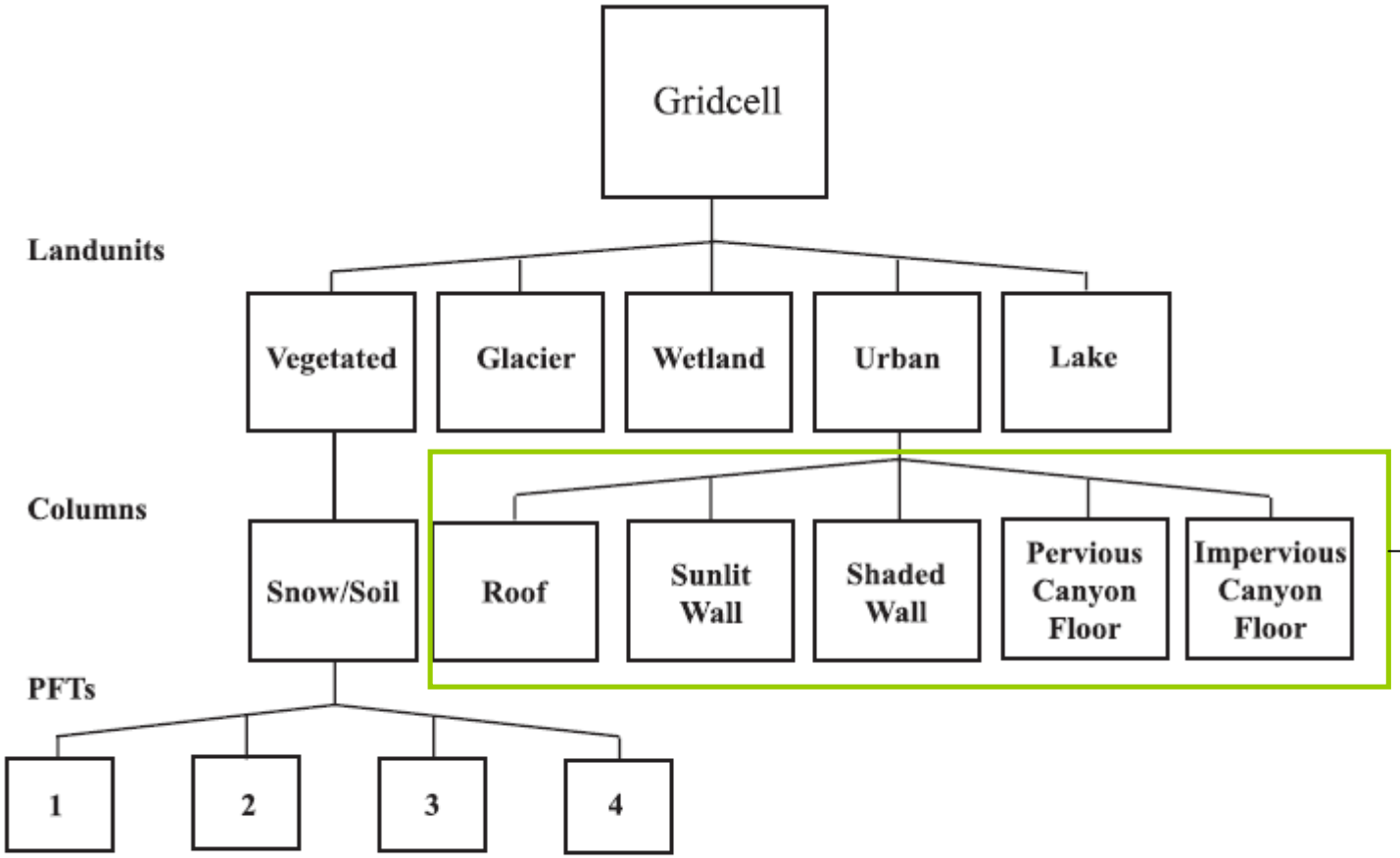

Urban

Canyon

FIG. 1. The CLM subgrid hierarchy emphasizing the vegetated and urban landunits. Grid cells are composed of landunits, snow–soil–urban columns, and plant functional types (PFTs). Four PFTS are shown here but up to 16 possible PFTs that differ in physiology and structure may coexist on a single column. Reproduced from Fig. 1 of Oleson et al. (2010a) with permission from John Wiley & Sons, Inc.

(Keith Oleson, 2011)

- **Attribution of UHI**

$$\Delta T = T_u - T_r \qquad (3)$$

$$\Delta T = C_R + C_H + C_{LE} + C_s + C_{AH} + e \qquad (4)$$

$$\Delta T \approx \underbrace{\frac{\lambda_0}{1+f}\Delta R_n^*}_{①} + \underbrace{\frac{-\lambda_0}{(1+f)^2}(R_n^* - Q_s + Q_{AH})\Delta f_1}_{②} + \underbrace{\frac{-\lambda_0}{(1+f)^2}(R_n^* - Q_s + Q_{AH})\Delta f_2}_{③} + \underbrace{\frac{-\lambda_0}{1+f}\Delta Q_s}_{④} + \underbrace{\frac{\lambda_0}{1+f}\Delta Q_{AH}}_{⑤} \qquad (5)$$

①: Radiation balance

②: Aerodynamic resistance (convection)

③: Bowen ratio

④: Heat storage

⑤: Anthropogenic heat addition

$$\lambda_0 = 1/4\varepsilon\sigma T^3$$

$$f = \frac{\lambda_0 \rho C_p}{r_a}(1+\frac{1}{\beta})$$

$$R_n^* = (1-\alpha)K_\downarrow + L_\downarrow - (1-\varepsilon)L_\downarrow - \varepsilon\sigma T_a^4$$

$$\Delta f_1 = \frac{-\lambda_0 \rho C_p}{r_a}(1+\frac{1}{\beta})\frac{\Delta r_a}{r_a}$$

$$\Delta f_2 = \frac{-\lambda_0 \rho C_p}{r_a}\frac{\Delta\beta}{\beta^2}$$

Results

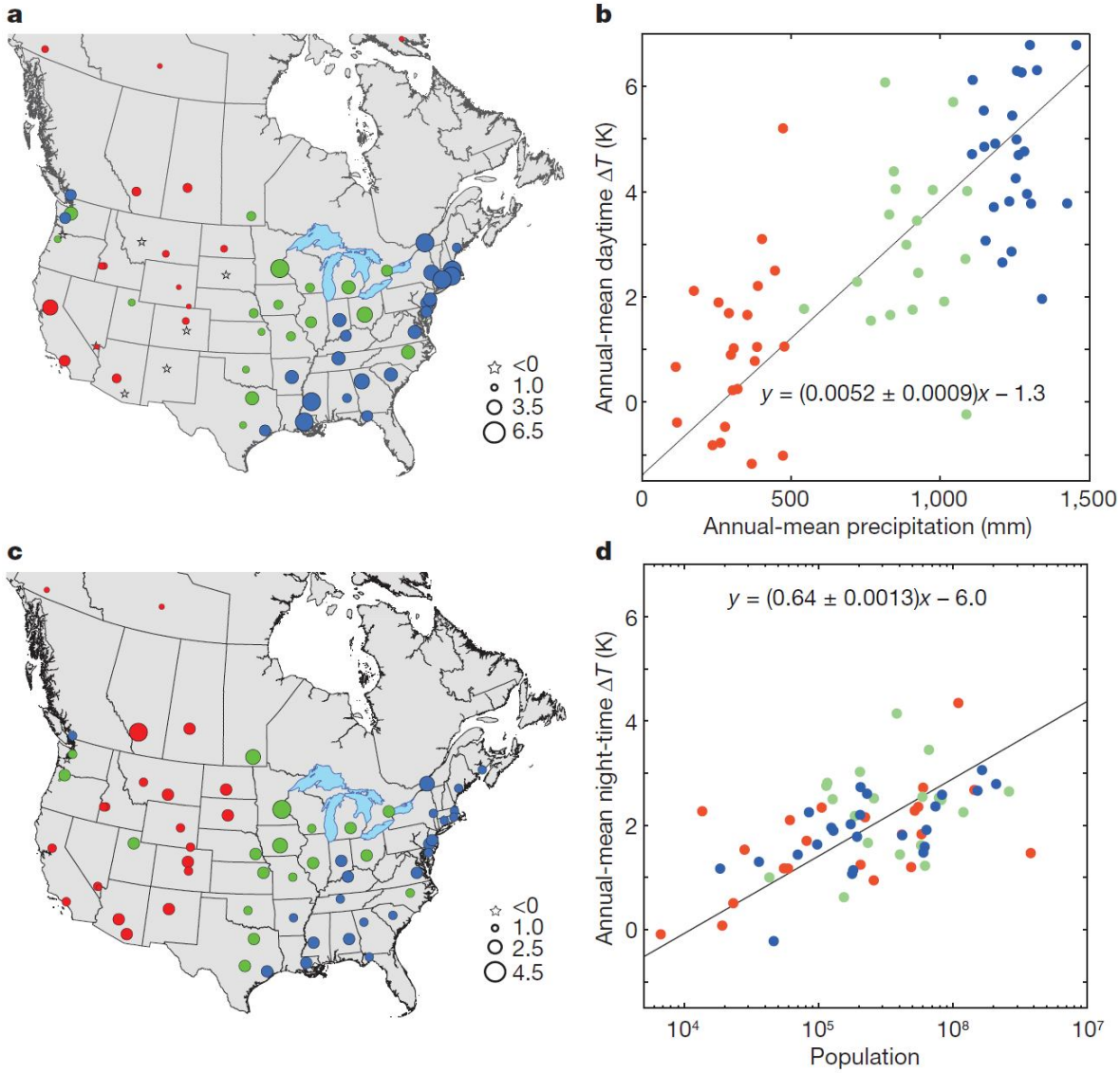

Figure 1 | Precipitation and population influences on MODIS-derived annual-mean UHI intensity. **a**, Map of daytime UHI (shown in K by symbol type/size). **b**, Dependence of daytime UHI on precipitation ($r = 0.74$, $P < 0.001$). **c**, Map of night-time UHI. **d**, Dependence of night-time UHI on population ($r = 0.54$, $P < 0.001$). Red, green and blue symbols denote cities with annual mean precipitations less than 500 mm, between 500 and 1,100 mm, and over 1,100 mm, respectively. Lines in **b** and **d** are linear regression fits to the data. Parameter bounds for the regression slope are the 95% confidence interval.

Aerodynamical resistance

e: rural land (39s m-1) < urban land (62 s m-1)

d: rural land (66s m-1) > urban land (53 s m-1)

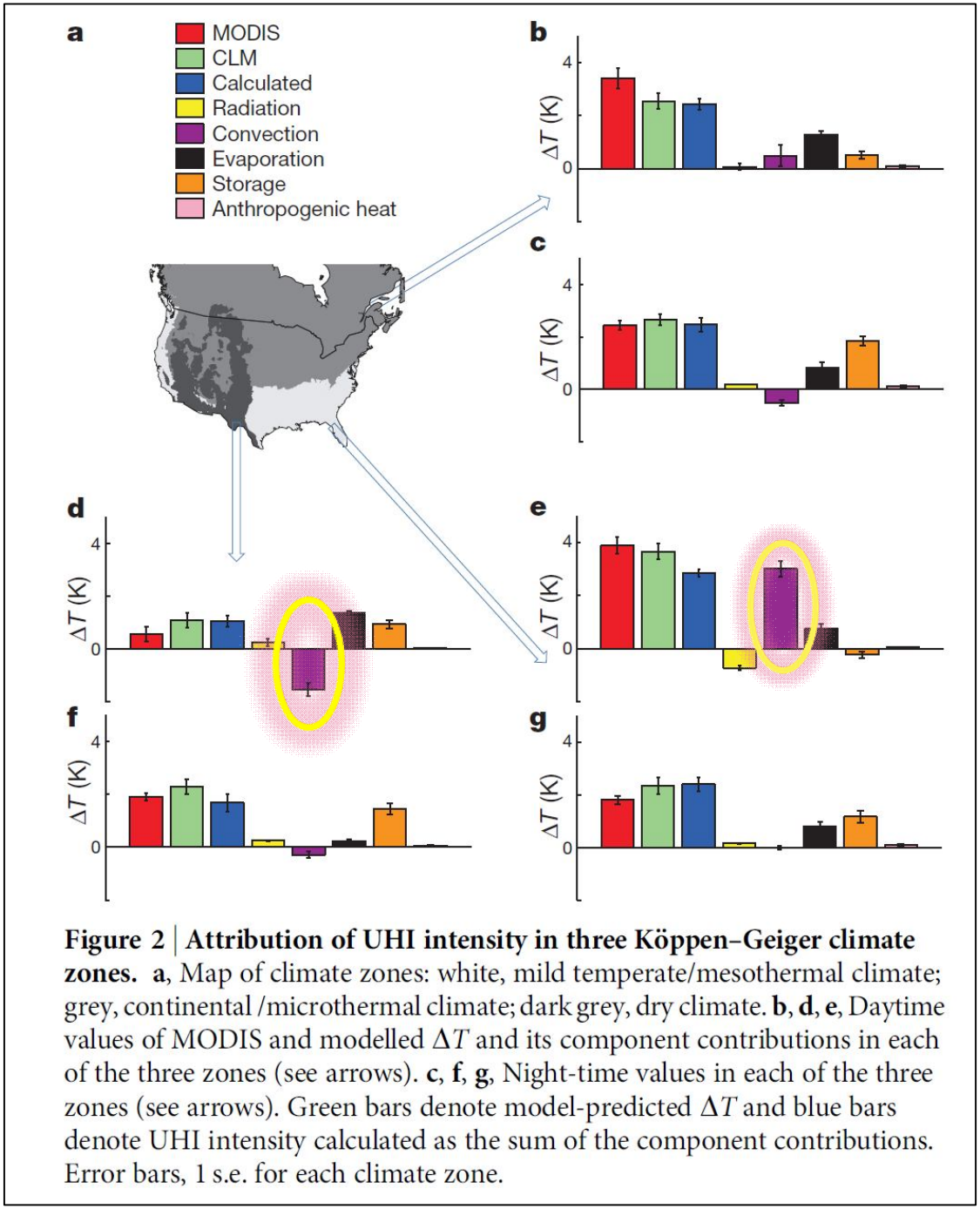

Figure 2 | Attribution of UHI intensity in three Köppen–Geiger climate zones. **a**, Map of climate zones: white, mild temperate/mesothermal climate; grey, continental /microthermal climate; dark grey, dry climate. **b**, **d**, **e**, Daytime values of MODIS and modelled ΔT and its component contributions in each of the three zones (see arrows). **c**, **f**, **g**, Night-time values in each of the three zones (see arrows). Green bars denote model-predicted ΔT and blue bars denote UHI intensity calculated as the sum of the component contributions. Error bars, 1 s.e. for each climate zone.

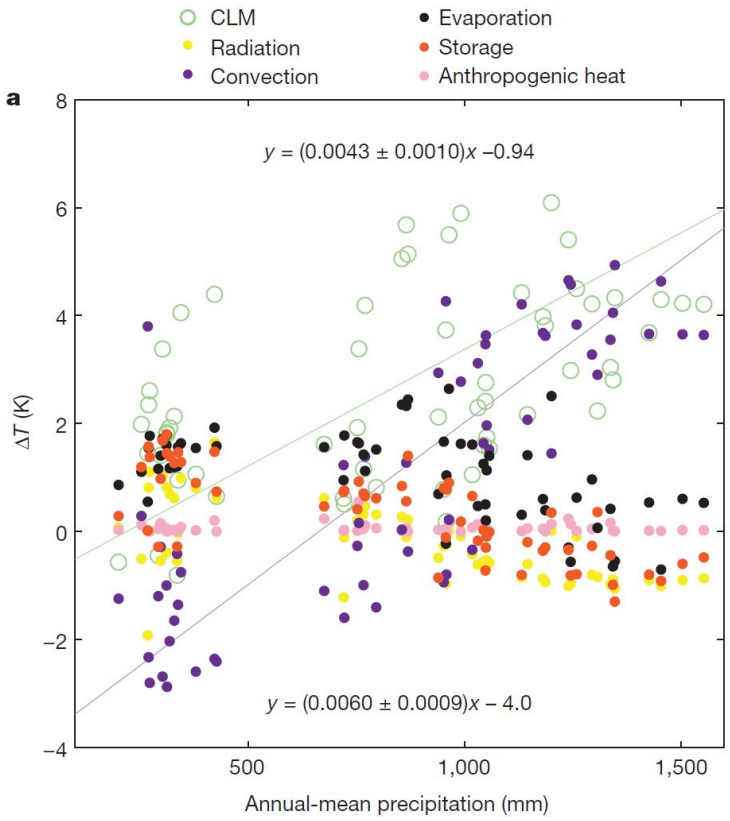

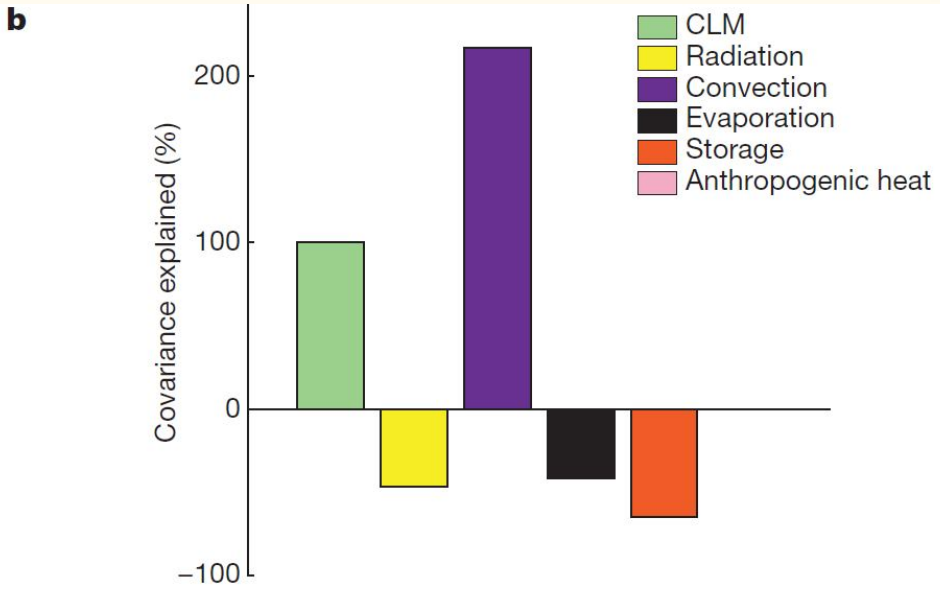

Figure 3 | Relationship between model-predicted daytime ΔT and precipitation among the cities. **a**, Correlation of ΔT and the individual biophysical components with annual-mean precipitation. Lines are linear regression fits to the corresponding data. Parameter bounds for the regression slope are the 95% confidence interval. **b**, ΔT–precipitation covariance explained by different biophysical factors. Note that the covariance explained by the anthropogenic heat term is negligibly small.

$$Cov(\Delta T,P)=Cov(C_R,P)+Cov(C_H,P)+Cov(C_{LE},P)+Cov(C_s,P)+Cov(C_{AH},P)+Cov(C_e,P) \quad (6)$$

"It is the changes in convection efficiency that control the daytime ΔT -precipitation spatial covariance among the cities."

Comparison between two cities

Identical morphological and biophysical specifications

Extended Data Table 1 | Urban parameters of a city pair in CLM

City	Richmond	Billings
State	Virginia	Montana
Latitude (°)	37.53	45.79
Longitude (°)	-77.42	-108.54
Canyon Height/Width	0.48	0.48
Mean building height (m)	12	12
Roof thickness (m)	0.15	0.15
Wall thickness (m)	0.28	0.28
Wind height in canyon (m)	6	6
Roof fraction	0.55	0.50
Pervious road fraction	0.66	0.64
Emissivity (Impervious road)	0.91	0.91
Emissivity (pervious road)	0.95	0.95
Emissivity (roof)	0.65	0.65
Emissivity (wall)	0.91	0.91
Albedo (Impervious road)	0.13	0.13
Albedo (pervious road)	0.08	0.08
Albedo (roof)	0.30	0.30
Albedo (wall)	0.34	0.34
Roof thermal conductivity ($W\ m^{-1}\ K^{-1}$)	0.84	0.84
Wall thermal conductivity ($W\ m^{-1}\ K^{-1}$)	1.06	1.06
Impervious road thermal conductivity ($W\ m^{-1}\ K^{-1}$)	1.67	1.67
Layers of impervious road	2	2
Roof heat capacity ($MJ\ m^{-3}\ K^{-1}$)	0.76	0.76
Wall heat capacity ($MJ\ m^{-3}\ K^{-1}$)	0.81	0.81
Impervious road heat capacity ($MJ\ m^{-3}\ K^{-1}$)	2.06	2.06

The sensitivity to precipitation

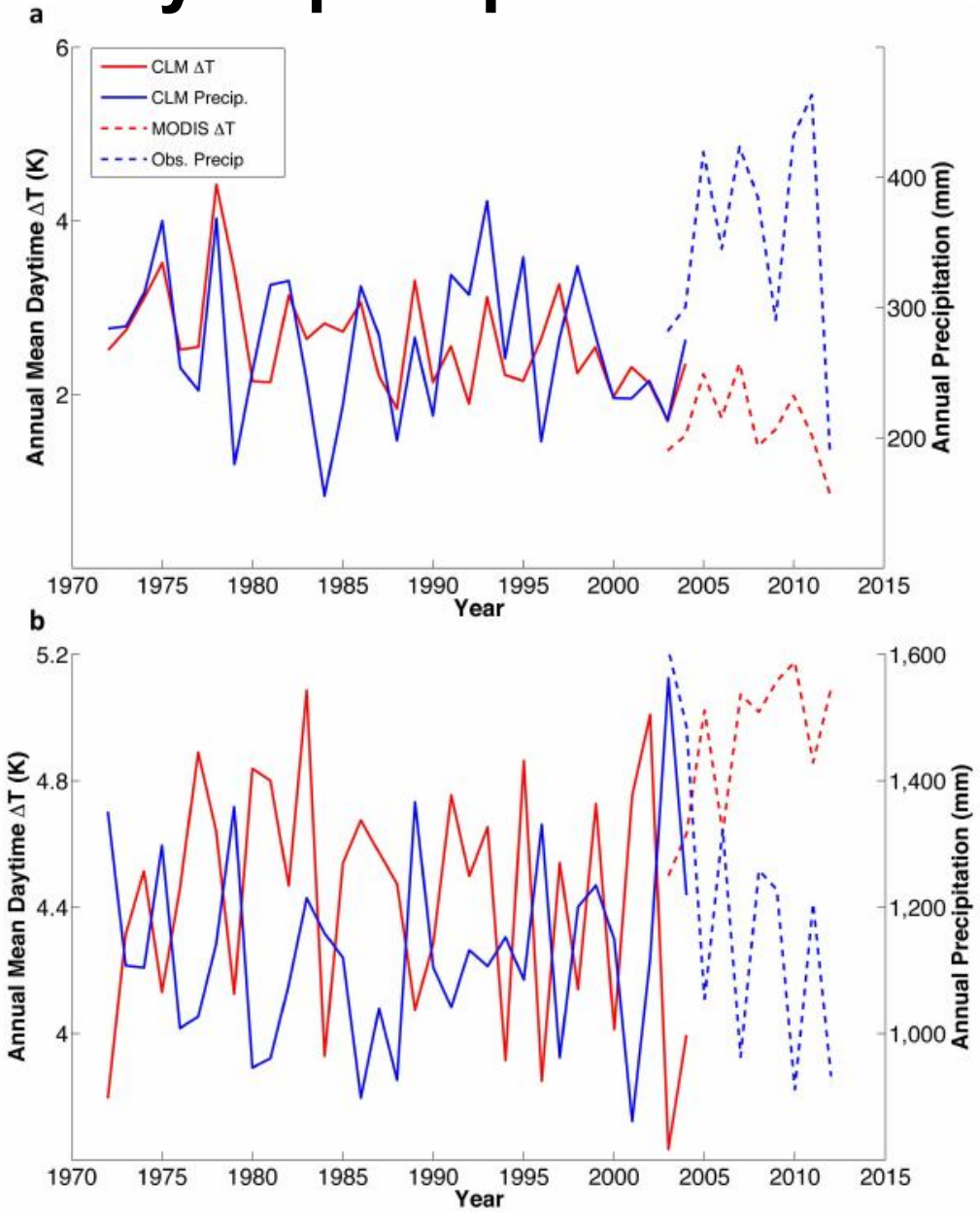

Billings (353mm)

Richmond (1183mm)

Extended Data Figure 2 | Time series of MODIS and model-predicted daytime ΔT and annual precipitation. a, Billings, Montana. b, Richmond, Virginia.

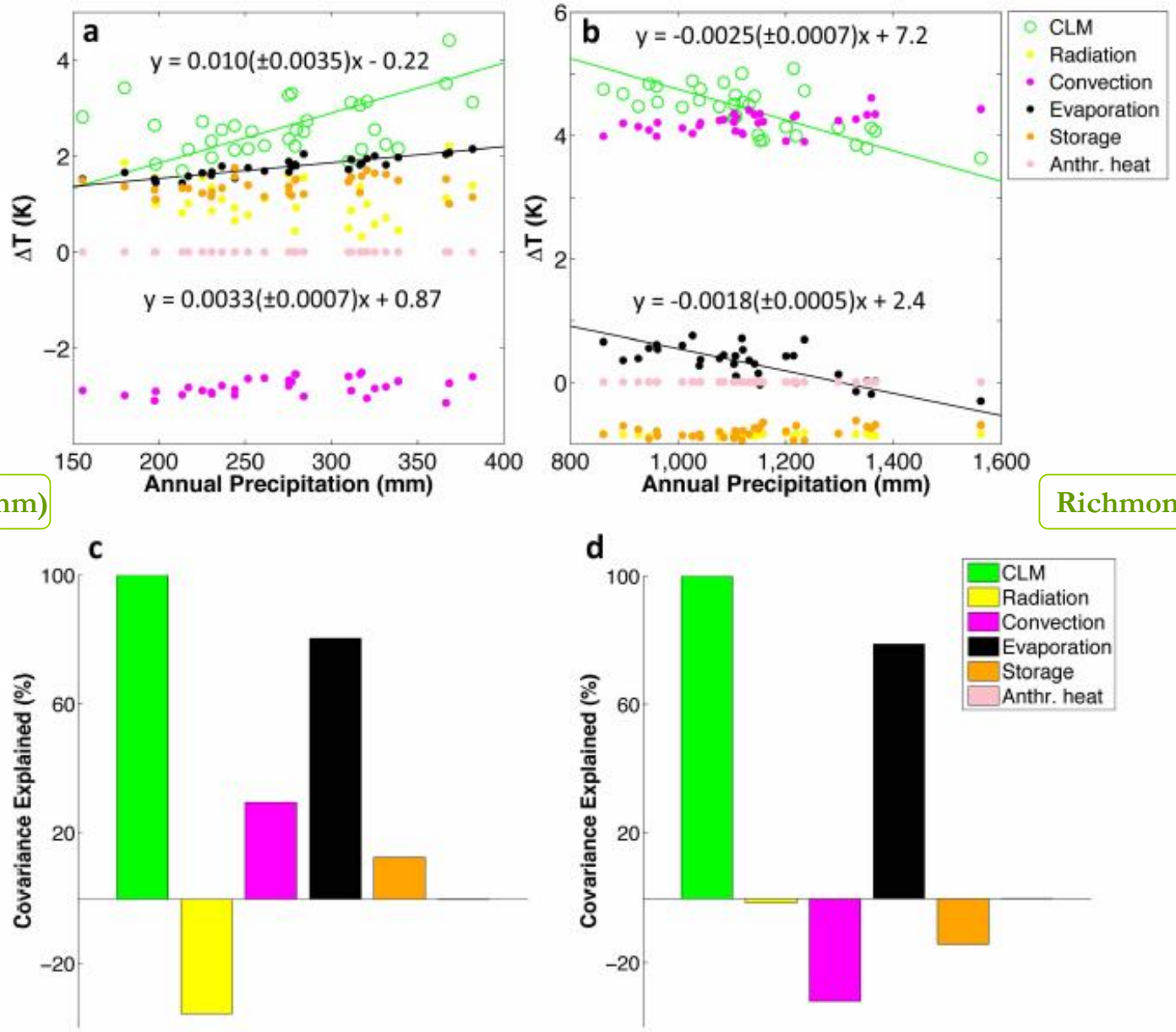

Extended Data Figure 3 | Relationship between interannual variations in model-predicted daytime ΔT and precipitation. a, Correlation of ΔT and the individual biophysical components with annual precipitation at Billings, Montana. **b**, Same as in a except for Richmond, Virginia. c, ΔT–precipitation temporal covariance explained by different biophysical factors at Billings, Montana. **d**, Same as in c except for Richmond, Virginia. Lines are best linear regression fits to the data points. Parameter bounds for the regression slope are the 95% confidence interval.

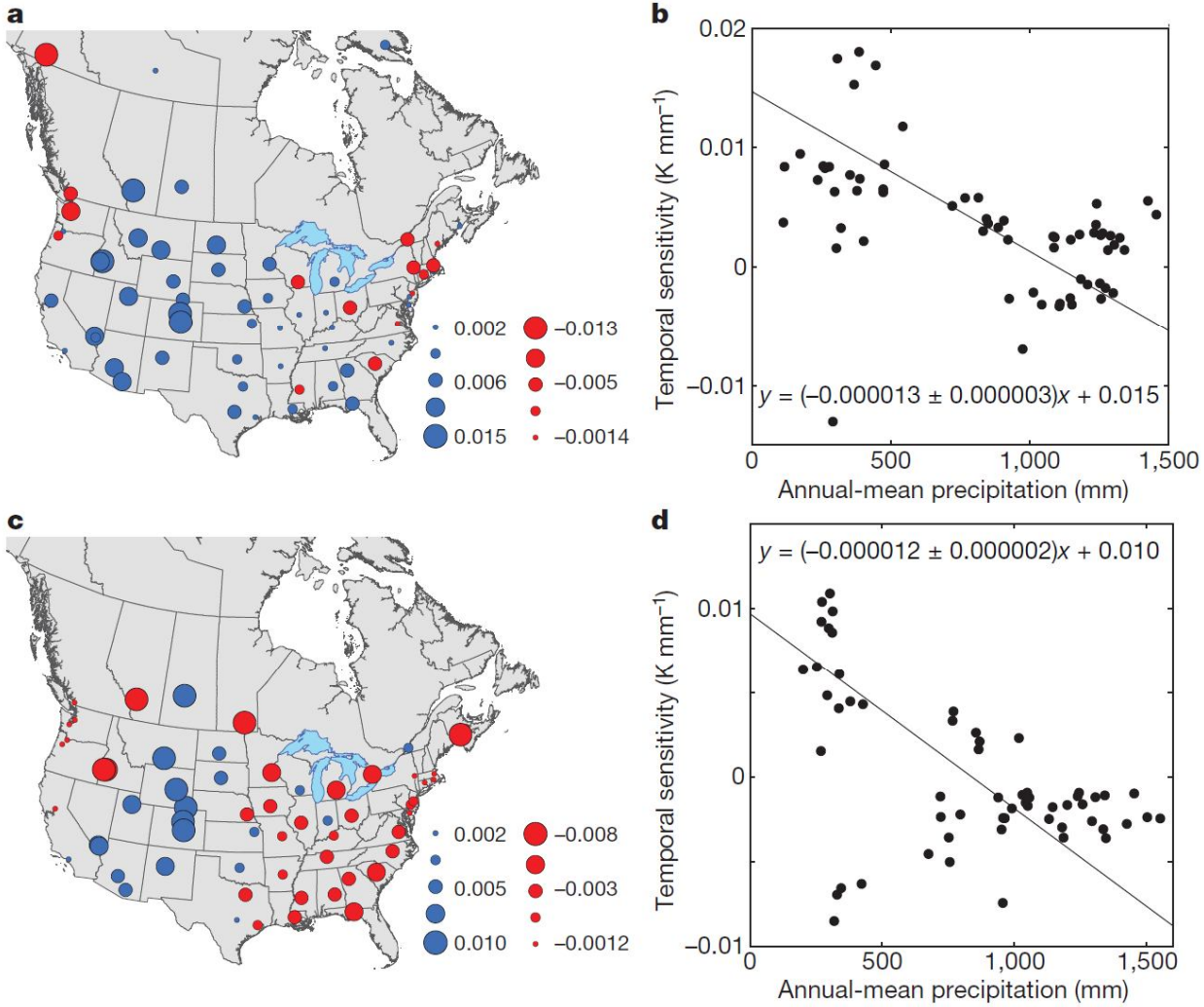

Figure 4 | Temporal sensitivity of UHI intensity to precipitation. **a**, **c**, Map of the temporal sensitivities (shown in K mm^{-1} by symbol size) according to MODIS (**a**) and the climate model (**c**). **b**, **d**, Dependence of MODIS (**b**) and model-predicted (**d**) temporal sensitivity on annual mean precipitation. The outlier city in the MODIS panels is Whitehorse in Yukon. The four outlier cities in the model panels are Boise and Nampa in Idaho, Winnipeg in Manitoba and Calgary in Alberta. Lines in **b** and **d** are linear regression fits to the data. Parameter bounds for the regression slope are the 95% confidence interval.

Mean value = **-0.0021**K mm^{-1} (eastern US)

Heatwave climatology

- Heatwave intensity: multiples of standard deviation of summertime temperature from climatological mean

$$\sigma \approx 0.6K \quad \text{(North American mean value)}$$

- For southeast US, daytime ΔT (3.9K) is equivalent to 7σ

- 500mm reduction in annual precipitation (**-0.0021**K mm^{-1}) ⟶ 1.1K or 2σ increase in daytime ΔT

Discussion

- Compared with other biophysical factors, increasing urban albedo can be a viable way to mitigate urban heat island.

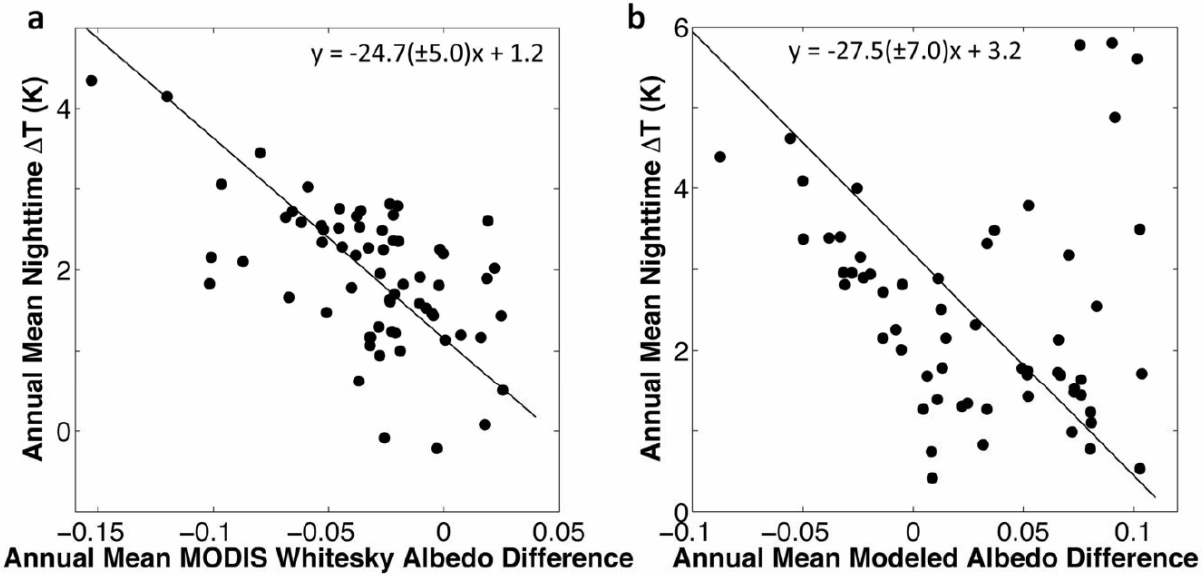

Extended Data Figure 4 | Albedo influence on annual mean night-time UHI intensity. **a**, Dependence of night-time MODIS-derived UHI on white-sky albedo difference (that is, urban albedo minus rural albedo; $r = -0.60$, $P < 0.001$). **b**, Dependence of night-time modelled UHI on modelled albedo difference ($r = -0.56$, $P < 0.001$ excluding four outliers; $r = -0.18$, $P = 0.16$ with all data points). The four outliers in the upper right corner of **b** are coastal cities (Olympia, Washington; Seattle, Washington; Salem, Oregon; Vancouver, British Columbia) that have high biases of the modelled ΔT compared to the MODIS ΔT. Lines are linear regression fits to the data. Parameter bounds for the regression slope are the 95% confidence interval.

Doctoral research design

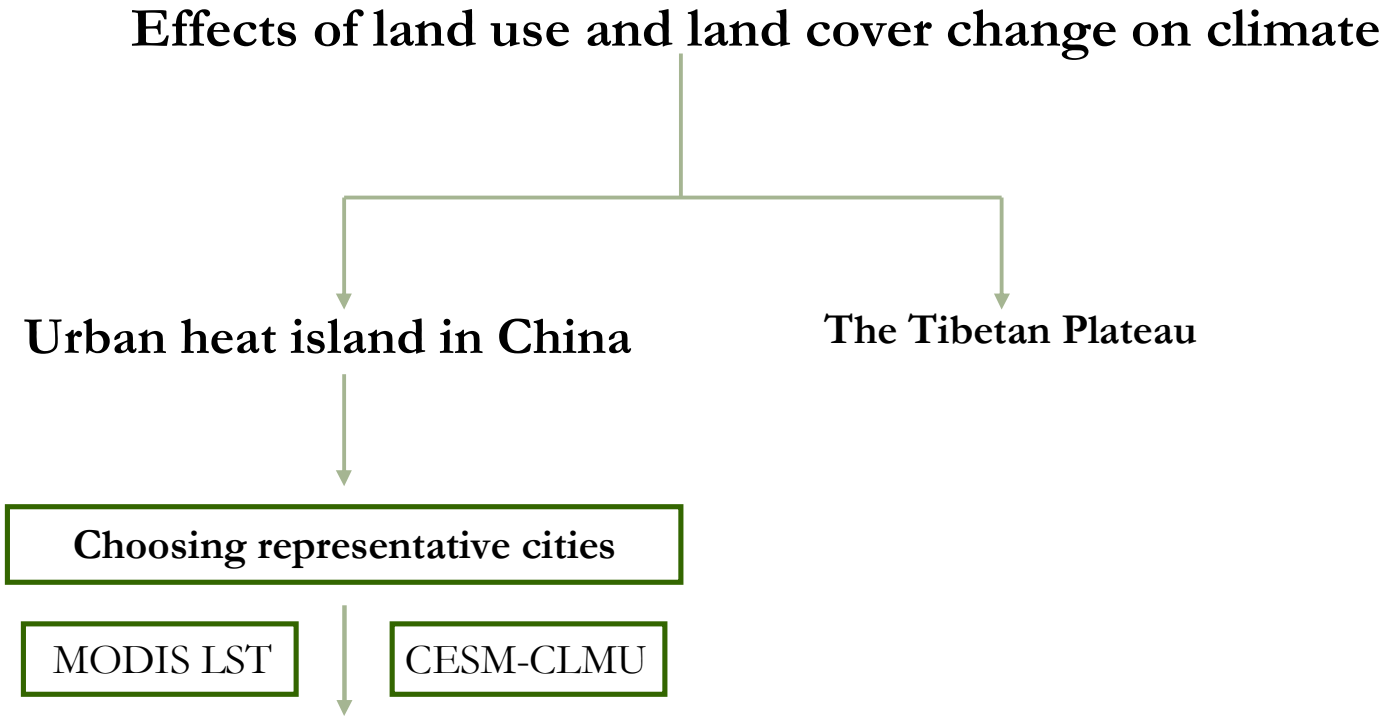

1) The mechanism forming daytime and night-time UHI

2) Separate the contributions of factors to UHI

3) Understand the effect of climatic context on UHI

Chosen cities in China

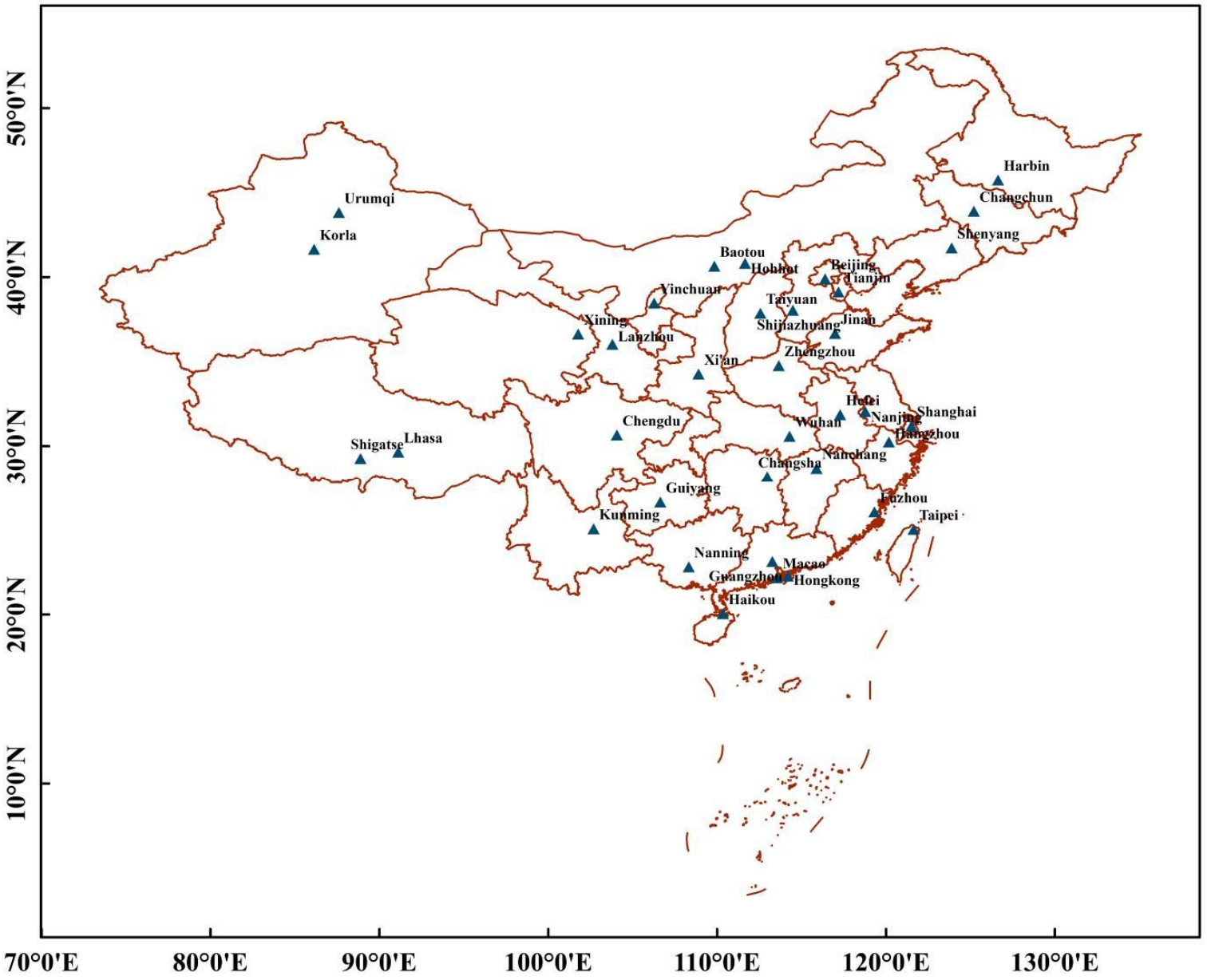

The Tibetan Plateau

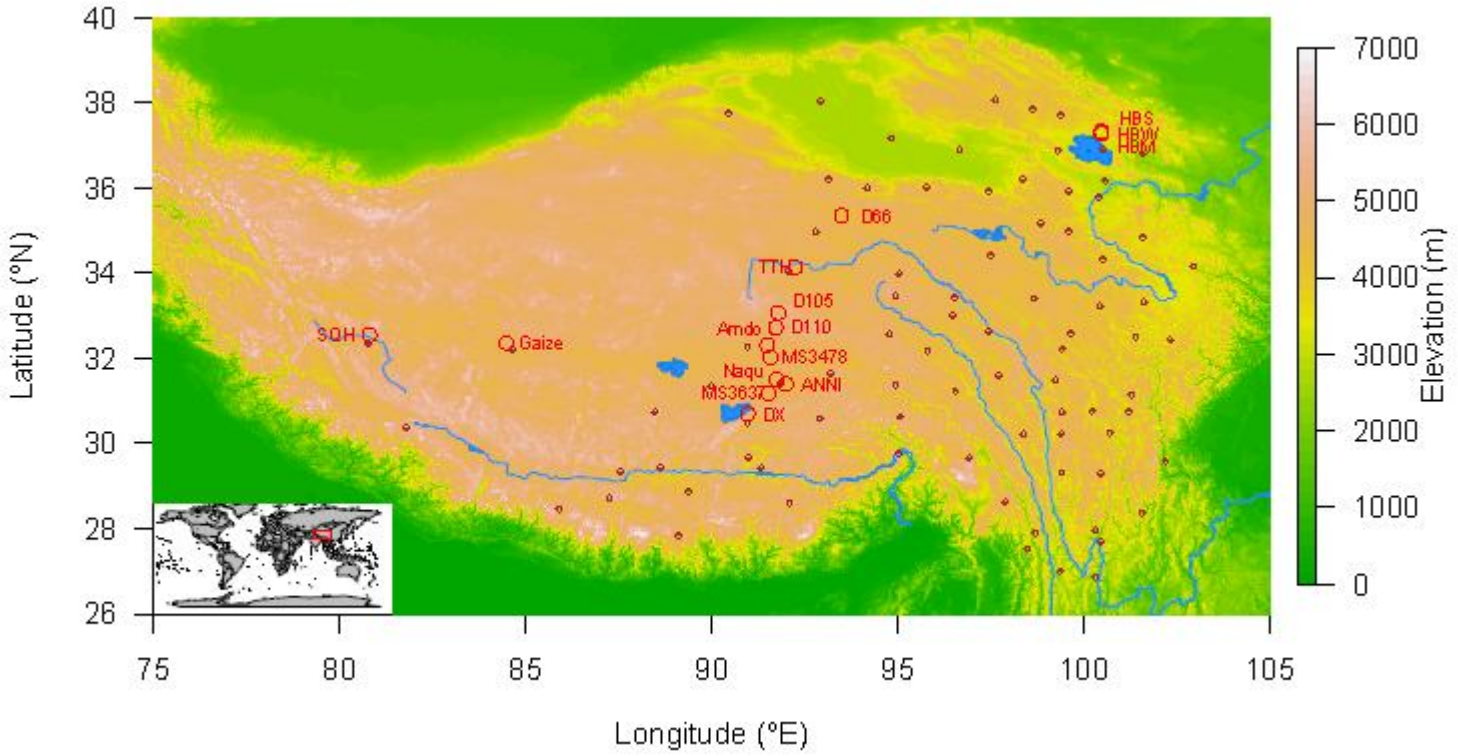

(Shi and Liang, 2014)

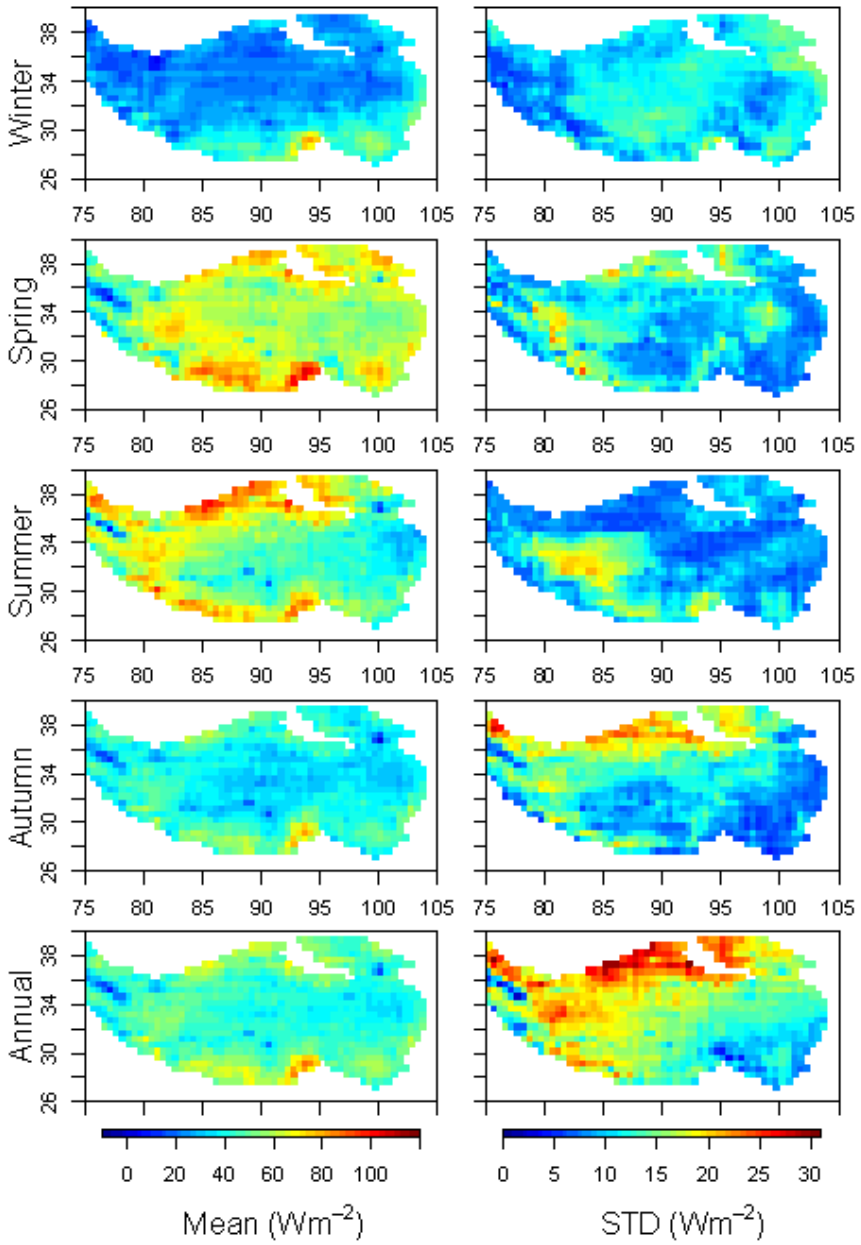

Figure 8. Spatial distribution of seasonal/annual mean and STD of the fused sensible heat flux over the TP (1984–2007). *(Shi and Liang, 2014)*

- The sensible heat flux reached the lowest value in winter and decreased with latitude.
- In spring, summer and autumn, the high values were located in the western plateau, the mountain ranges and basins of the western plateau, and the Himalaya ranges in the south TP, respectively.
- The sensible heat flux was lower in summer than that in spring in the eastern TP.

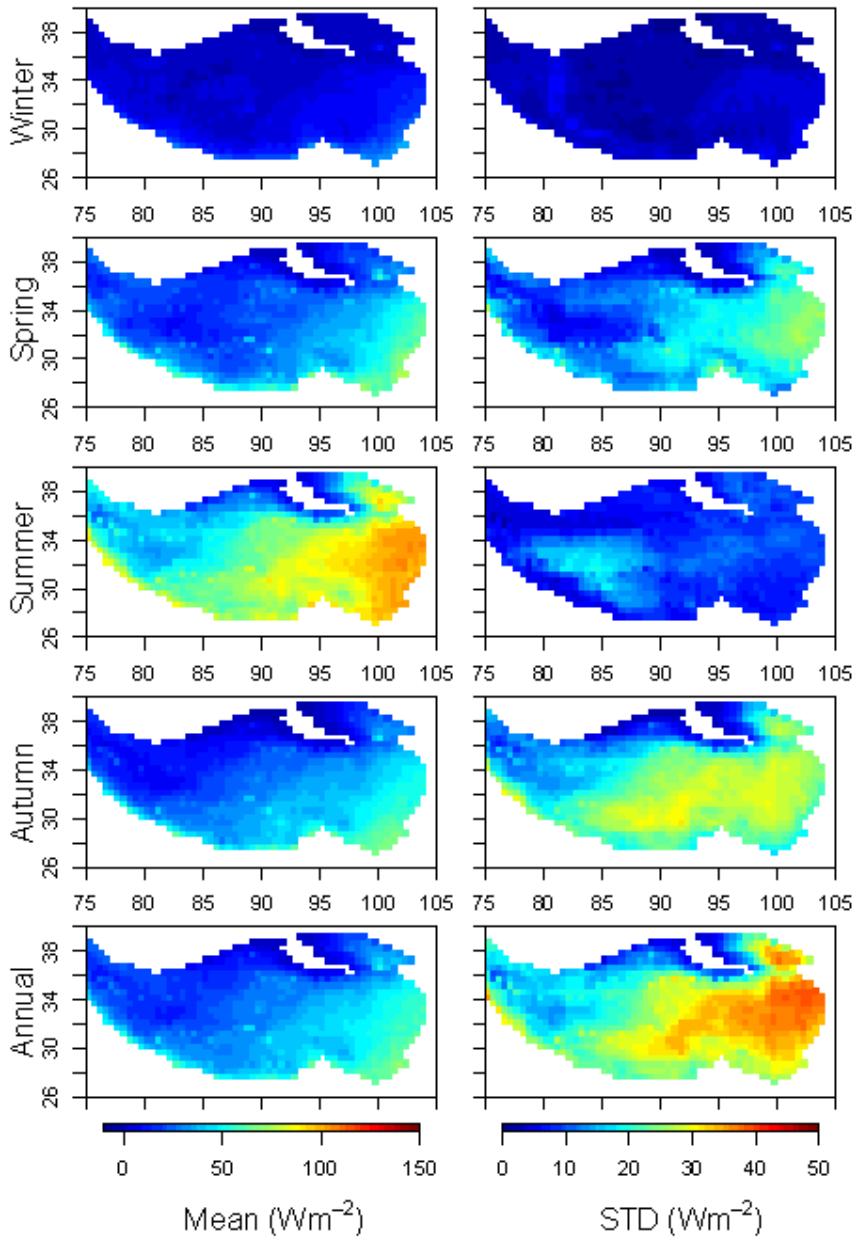

Figure 9. Spatial distribution of the seasonal/annual mean and STD of the fused latent heat flux over the TP (1984–2007). *(Shi and Liang, 2014)*

- The latent heat flux increased from northwest to southeast over the TP in all seasons.
- In summer, the high values were located in the eastern TP and in the South boundaries.

Warming: GHGS and black soot

(Xu et al, 2009)

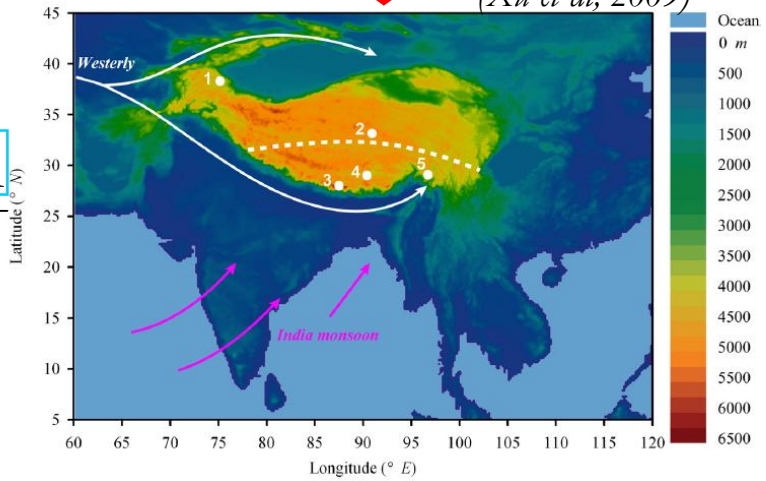

East Asia monsoon

Mechanical

Thermal

"Sensible-heat driven air pump"

Glaciers Melting

Albedo Change

Degrading Permafrost

(Qiu, 2008)

MODIS Albedo (3 Tibet sites)

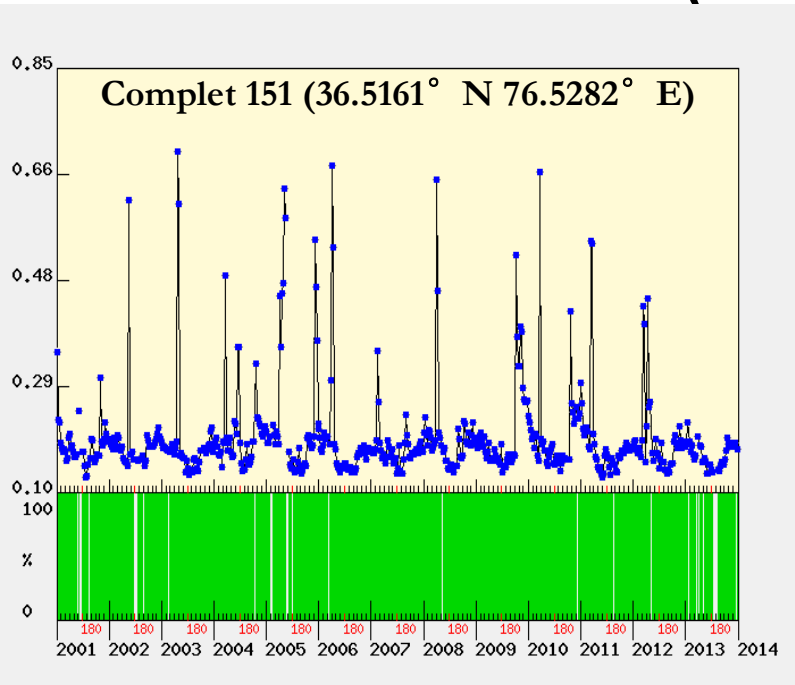

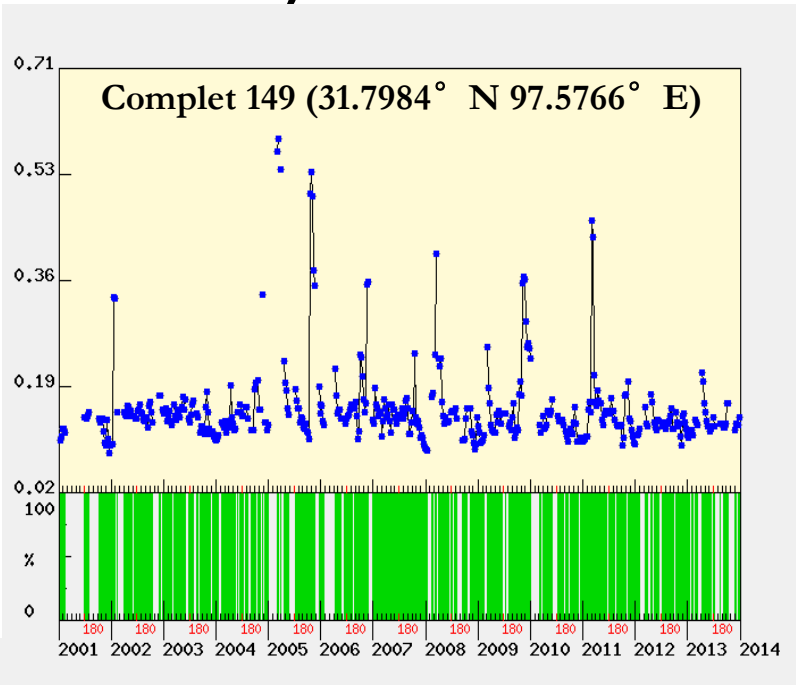

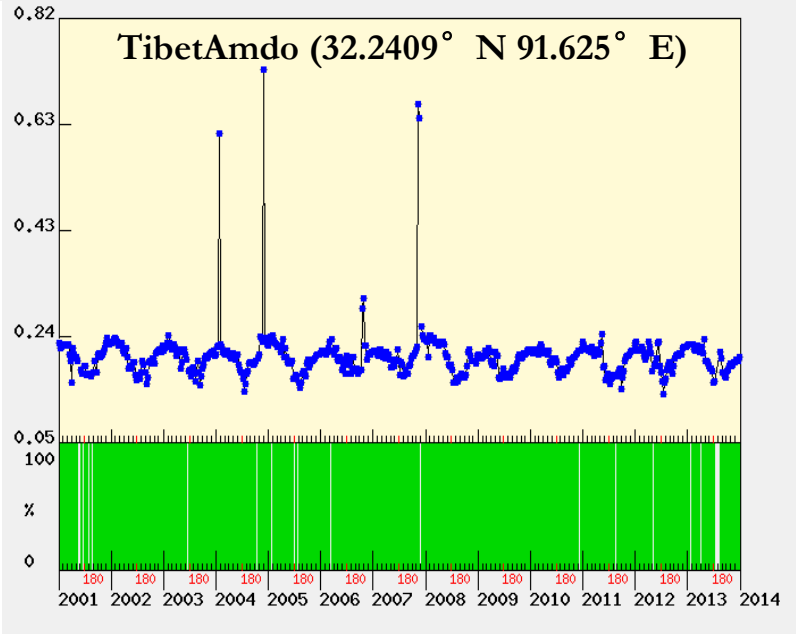

Monthly mean albedo (2001-2012)

Winter

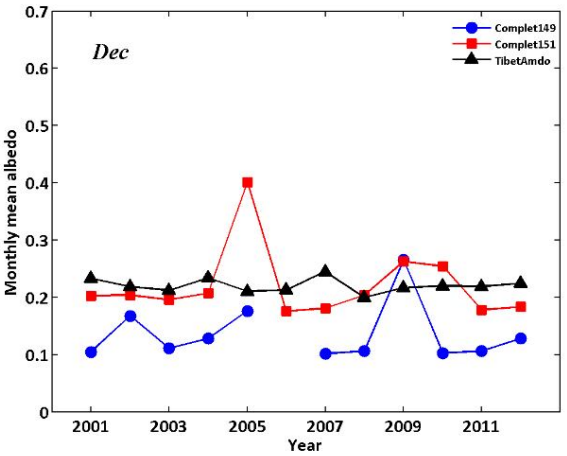

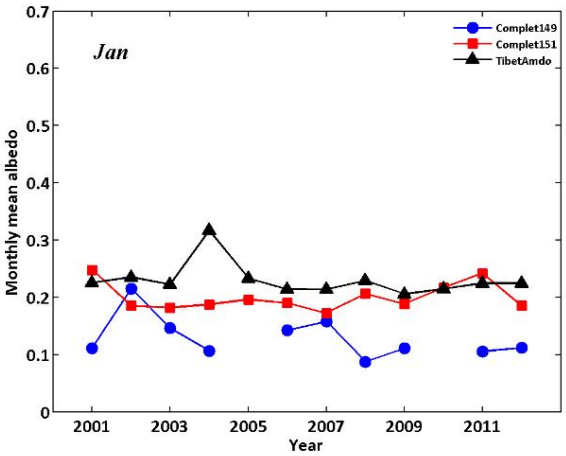

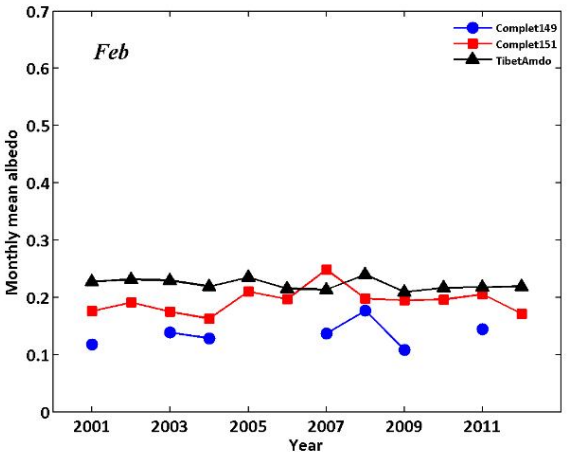

Spring

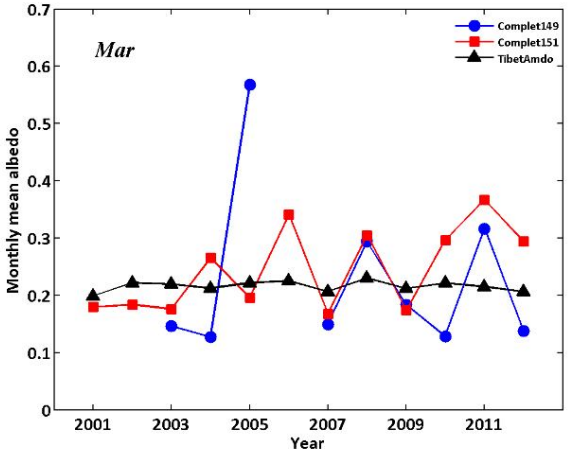

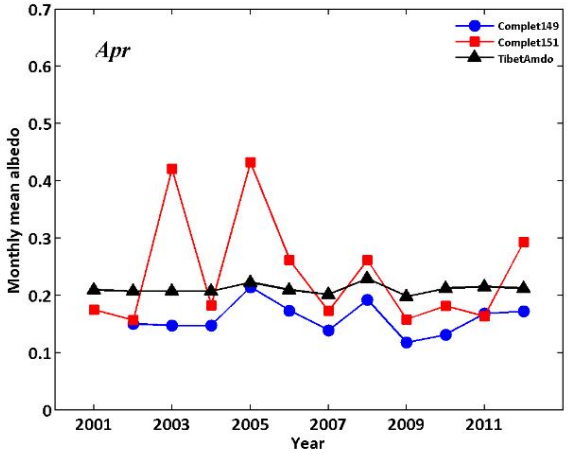

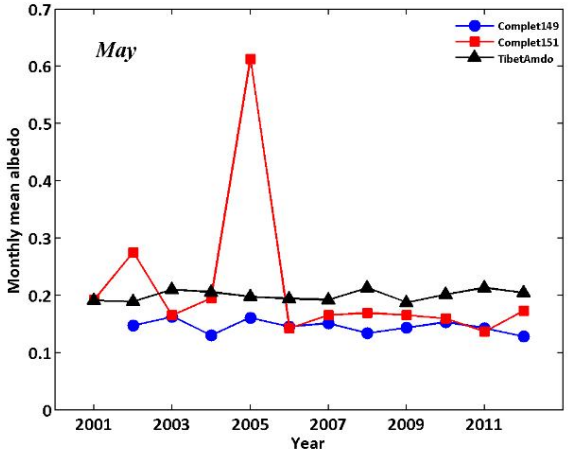

Summer

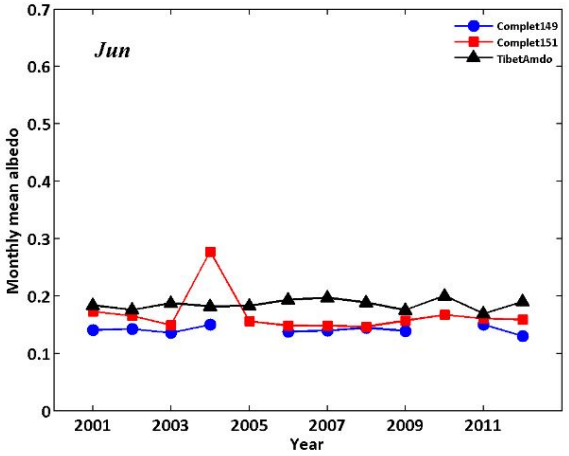

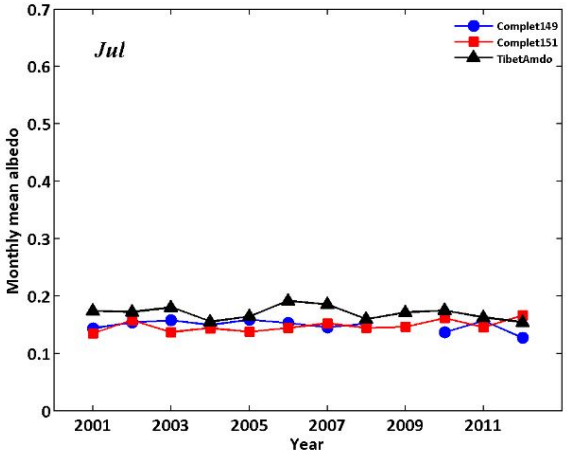

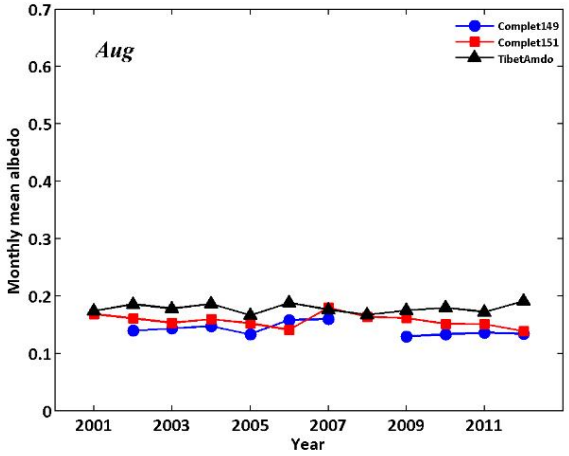

Autumn

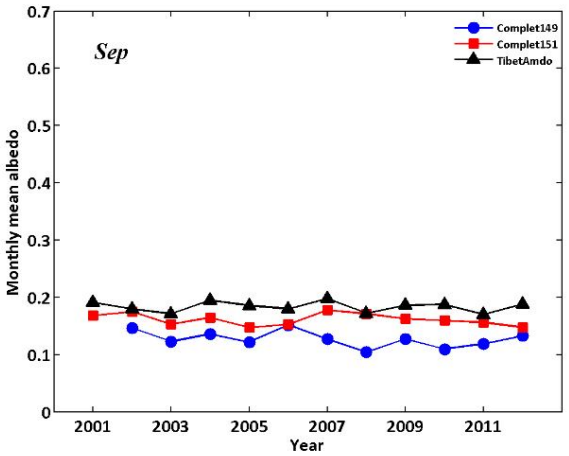

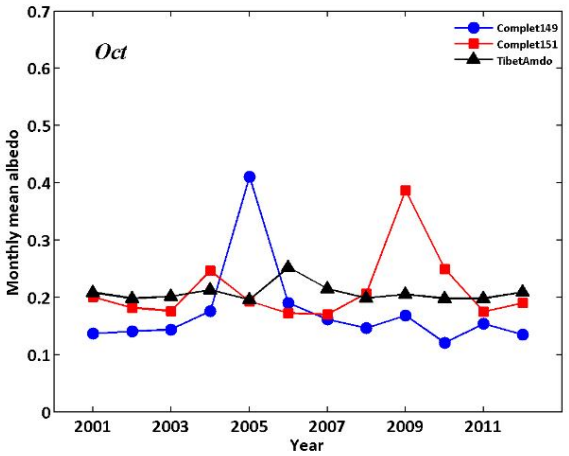

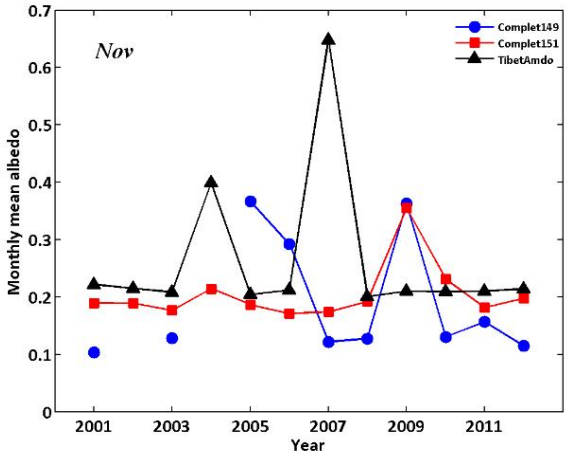


Thank
you